

The turbulent pressure of magnetoconvection for slow and rapid rotation

M. KÜKER¹ AND G. RÜDIGER¹

¹*Leibniz-Institut für Astrophysik Potsdam (AIP), An der Sternwarte 16, 14482 Potsdam, Germany*

ABSTRACT

Motivated by recent simulations of sunspot formation, we extend the theory of the pressure difference between magnetized and non-magnetized gas by Dicke to include rotating turbulence. While the (vertical) background field provides a positive-definite magnetic pressure difference between the magnetized and the unmagnetized gas, Reynolds stress and Maxwell stress of turbulence strongly modify this result. With the quasilinear approximation we demonstrate that the influence of the turbulence differs between the high-conductivity and the low-conductivity limits. Sufficiently small magnetic Reynolds numbers lead to magnetic pressure suppression where indeed the pressure excess can even assume negative values. Box simulations of magnetoconvection subject to a vertical magnetic field carried out with the Nirvana code confirm this overall picture. They also demonstrate how a global rotation *reduces* the negative magnetic pressure effect. For rapid rotation the total magnetic pressure difference caused by large-scale magnetic fields and turbulence even fully disappears for small field strengths. Magnetic fields of moderate strength thus neither reduce nor enhance the turbulence pressure of rapidly rotating convection. Consequences of this phenomenon for the star formation efficiency are shortly discussed.

Keywords: Magnetohydrodynamics (MHD) – Magnetic fields – rotation – convection – sunspots

1. INTRODUCTION

If in a fluid a magnetized domain exists with a non-magnetic surrounding in quasistationary equilibrium and the magnetic field has a cylindrical geometry $\mathbf{B} = (0, 0, B_0(R, \phi))$ then the gas pressure and the temperature differences between the inner and the outer regions will simply be

$$\delta P = -\frac{B_0^2}{2\mu_0}, \quad \delta T = -\frac{B_0^2}{2\mu_0} \frac{T}{P}, \quad (1)$$

(Dicke 1970). The magnetic domain is thus cooler than its non-magnetic surrounding. This straightforward explanation of the sunspot phenomenon fails, however, in one basic respect. Both the magnetized domain *and* its non-magnetic surrounding are turbulent. The large-scale Maxwell stress – which was the only one considered by Dicke – has thus to be completed by the Reynolds stress and the small-scale Maxwell stress caused by the overall convection. Instead of (1) we write

$$P_{\text{in}} = P_{\text{ext}} - \delta P^{\text{tot}}, \quad (2)$$

where P_{in} is the pressure in the magnetic region, P_{ext} the pressure outside the magnetic region, and the second term on

the right hand side collects the contributions from Reynolds stress and Maxwell stress. Note that the sign of δP^{tot} is not known from the definition. Positive values cause the gas pressure of the magnetized fluid to be reduced compared with the external pressure as described by Eq. (1). If, however, $\delta P^{\text{tot}} < 0$ would occur because of the influence of turbulence, then the inner gas pressure would exceed the external gas pressure, with consequences recently described by Losada et al. (2017) with respect to the theory of sunspot formation. Our computations confirm the existence of this phenomenon, provided the magnetic field is not too strong, the rotation not too rapid, and the electric conductivity not too high. We find that rapid rotation leads to $\delta P^{\text{tot}} \simeq 0$, so that the inner gas pressure approaches the outer gas pressure, which according to the second relation in (1) will also be true for the temperature.

In the following we derive both the turbulence-originated Reynolds stresses and the Maxwell stresses for a turbulent fluid rotating with an angular velocity $\boldsymbol{\Omega}$ under the presence of a uniform background field \mathbf{B} . The magnetic field will here be considered as vertical, i.e. as antiparallel to the density gradient. The fluctuating flow and field components are denoted by \mathbf{u} and by \mathbf{b} , resp. The standard Maxwell stress tensor

$$M_{ij} = \frac{1}{\mu_0} B_i B_j - \frac{1}{2\mu_0} \mathbf{B}^2 \delta_{ij} \quad (3)$$

of the considered MHD turbulence turns into the generalized stress tensor

$$M_{ij}^{\text{tot}} = M_{ij} - \rho Q_{ij} + M_{ij}^{\text{T}}, \quad (4)$$

with the one-point correlation tensor

$$Q_{ij} = \langle u_i(\mathbf{x}, t) u_j(\mathbf{x}, t) \rangle \quad (5)$$

of the flow and the turbulence-induced Maxwell stress tensor

$$M_{ij}^{\text{T}} = \frac{1}{\mu_0} \langle b_i(\mathbf{x}, t) b_j(\mathbf{x}, t) \rangle - \frac{1}{2\mu_0} \langle \mathbf{b}^2(\mathbf{x}, t) \rangle \delta_{ij}. \quad (6)$$

The terms with the Kronecker deltas in (4) form the total pressure. We write the one-point correlation tensor (5) for homogeneous and isotropic turbulence as

$$Q_{ij} = q_1 \delta_{ij} + q_2 \Omega_i \Omega_j + q_3 B_i B_j. \quad (7)$$

Each part of this tensor must be even in Ω and even in \mathbf{B} , there are no mixed elements. Only q_1 is thus relevant for the pressure evaluation. Similarly, for the Maxwell stress tensor, i.e.

$$B_{ij} = Q_1 \delta_{ij} + Q_2 \Omega_i \Omega_j + Q_3 B_i B_j, \quad (8)$$

so that for the pressure

$$\frac{P^{\text{tot}}}{\rho} = q_1 - \frac{Q_1}{\mu_0 \rho} + \frac{B_0^2}{2\mu_0 \rho} + \frac{1}{2\mu_0 \rho} (\langle b_x^2 + b_y^2 + b_z^2 \rangle) \quad (9)$$

results. The orientation of the vectors Ω and \mathbf{B} defines the model. A *vertical* magnetic background field is considered which shows in the positive radial (z) direction¹, $\mathbf{B} = B_0 (0, 0, 1)$. The angle θ between the rotation vector and the gravity defines the components of the rotation vector $\Omega = \Omega (-\sin \theta, 0, \cos \theta)$. From (7) one obtains

$$\langle u_x^2 \rangle = q_1 + q_2 \Omega^2 \sin^2 \theta, \quad \langle u_y^2 \rangle = q_1 + q_2 \Omega^2 \cos^2 \theta, \quad (10)$$

and from (8)

$$\langle b_x^2 \rangle = Q_1 + Q_2 \Omega^2 \sin^2 \theta, \quad \langle b_y^2 \rangle = Q_1 + Q_2 \Omega^2 \cos^2 \theta. \quad (11)$$

Hence

$$\begin{aligned} \frac{P^{\text{tot}}}{\rho} &= \frac{\cos^2 \theta \langle u_x^2 \rangle - \sin^2 \theta \langle u_y^2 \rangle}{\cos^2 \theta - \sin^2 \theta} \\ &+ \frac{B_0^2}{2\mu_0 \rho} + \frac{\langle b_x^2 + b_y^2 + b_z^2 \rangle}{2\mu_0 \rho} \\ &- \frac{1}{\mu_0 \rho} \frac{\cos^2 \theta \langle b_x^2 \rangle - \sin^2 \theta \langle b_y^2 \rangle}{\cos^2 \theta - \sin^2 \theta}. \end{aligned} \quad (12)$$

¹ x shows in meridional direction, y in azimuthal direction

Without rotation this expression simplifies to

$$\frac{P^{\text{tot}}}{\rho} = \langle u_x^2 \rangle + \frac{1}{2\mu_0 \rho} B_0^2 + \frac{1}{2\mu_0 \rho} \langle b_y^2 + b_z^2 - b_x^2 \rangle \quad (13)$$

(Rüdiger et al. 2013). Because of the isotropy in the horizontal plane we have $\langle b_y^2 + b_z^2 - b_x^2 \rangle = \langle b_z^2 \rangle$. All terms on the RHS of (13) are thus positive. For large magnetic background fields the middle term will exceed the other terms and for large magnetic Reynolds numbers the last term will dominate. Nevertheless, for weak fields and magnetic Reynolds numbers not too large it happens that the magnetic quenching of the first term in (13) provides so small intensities that the total magnetic-influenced pressure becomes smaller than the turbulence intensity $\langle u_x^{(0)2} \rangle$ hence for the gas pressure $P_{\text{in}} > P_{\text{ext}}$ instead of (1) which has been called the negative-pressure phenomenon (Brandenburg et al. 2010, 2011, 2012). In the simplest geometry after (1) then also $T_{\text{in}} > T_{\text{ext}}$ holds for the temperature.

With both analytical and direct numerical simulations Losada et al. (2013) calculated the total magnetic pressure (9) for driven turbulence with weak horizontal magnetic fields under the presence of global rotation. The rotation, however, was too slow for the numerical simulations to show trends for suppression or amplification of the total magnetic-influenced turbulence pressure (their Fig. 1).

2. DRIVEN TURBULENCE

The influences of the magnetic field and the basic rotation on driven turbulence are similar but not identical. While the magnetic field always reduces the velocity components perpendicular to the magnetic field this is not obvious for rotation (Chandrasekhar 1961). In order to demonstrate this situation we shall in the following formulate a quasilinear theory of the modifications a turbulence field driven by a fluctuating force field undergoes through the combined action of a uniform magnetic field and solid-body rotation. For simplicity the magnetic field may be aligned with the rotation axis. Because of the structure of the pressure equation (13) we are particularly interested in results for the transverse intensity $\langle u_x^2 \rangle$ when the magnetic field and the rotation axis define the z -axis.

It is almost trivial that within this concept the signs of Ω and \mathbf{B} do not play any role. The Fourier component of the velocity field in the rotating system under the influence of magnetic fields can be expressed via

$$\hat{u}_i(\mathbf{k}, \omega) = D_{ij} \hat{u}_j^{(0)}(\mathbf{k}, \omega) \quad (14)$$

by the Fourier component of the driven turbulence $\hat{u}^{(0)}(\mathbf{k}, \omega)$. The tensor D_{ij} for the simultaneous influence of global rotation and magnetic field,

$$D_{ij} = \frac{N \delta_{ij} + W \epsilon_{ijl} k_l^{\circ}}{N^2 + W^2}, \quad (15)$$

has been given by [Kitchatinov et al. \(1994\)](#). Here N carries the impact of the magnetic field and W that of the global rotation. In detail it is

$$N = 1 + \frac{(\mathbf{k} \cdot \mathbf{V}_A)^2}{(-i\omega + \nu k^2)(-i\omega + \eta k^2)},$$

$$W = \frac{2(\mathbf{k}^\circ \cdot \boldsymbol{\Omega})}{-i\omega + \nu k^2}. \quad (16)$$

As required, all terms are invariant against the transformation $\mathbf{B} \rightarrow -\mathbf{B}$, the sign of the magnetic field does not play any role. ν is the microscopic viscosity, $\eta = 1/\mu_0\sigma$ the magnetic resistivity, σ the electric conductivity and $V_A = B_0/\sqrt{\mu_0\rho}$ the Alfvén velocity. $\mathbf{k}^\circ = \mathbf{k}/k$ is a unit vector.

For homogeneous and isotropic turbulence with its spectral tensor,

$$\hat{Q}_{ij}^{(0)}(\mathbf{k}, \omega) = \frac{E(k, \omega)}{16\pi k^2} (\delta_{ij} - k_i^\circ k_j^\circ), \quad (17)$$

we find after some algebra that

$$\hat{Q}_{ij}(\mathbf{k}, \omega) = \frac{E(k, \omega)}{16\pi k^2 (N^2 + W^2)(N^{*2} + W^{*2})} \times$$

$$[(NN^* + WW^*)(\delta_{ij} - k_i^\circ k_j^\circ) + (N^*W - NW^*)\epsilon_{ijl}k_l^\circ] \quad (18)$$

with the asterisk for complex conjugate expressions. The local spectrum E is defined by

$$\langle \mathbf{u}^2 \rangle = \int_0^\infty \int_0^\infty E(k, \omega) dk d\omega. \quad (19)$$

For weak fields and slow rotation it is thus enough to consider the correlation tensor in the first order of B_0^2 and Ω^2 . One finds

$$\langle u_x^2 \rangle - \langle u_x^{(0)2} \rangle = \iiint (k_y^2 + k_z^2) \left(\frac{3\omega^2 - \nu^2 k^4}{(\omega^2 + \nu^2 k^4)^2} (2\mathbf{k} \cdot \boldsymbol{\Omega}/k)^2 + \right.$$

$$\left. + \frac{2(\omega^2 - \nu\eta k^4)}{(\omega^2 + \nu^2 k^4)(\omega^2 + \eta^2 k^4)} (\mathbf{k} \cdot \mathbf{V}_A)^2 \right) \times$$

$$\frac{E}{16\pi k^4} d\mathbf{k} d\omega, \quad (20)$$

which for $\nu = \eta$ can also be written as

$$\langle u_x^2 \rangle - \langle u_x^{(0)2} \rangle = \frac{1}{16\pi} \iiint \frac{k_y^2 + k_z^2}{k^4}$$

$$\left(\frac{\omega}{(\omega^2 + \nu^2 k^4)^2} \frac{\partial(\omega^2 + \nu^2 k^4)E}{\partial\omega} (2\mathbf{k} \cdot \boldsymbol{\Omega}/k)^2 + \right.$$

$$\left. + \frac{2\omega}{\omega^2 + \eta^2 k^4} \frac{\partial E}{\partial\omega} (\mathbf{k} \cdot \mathbf{V}_A)^2 \right) d\mathbf{k} d\omega. \quad (21)$$

The coefficients of both terms are different. The influences of rotation and magnetic field onto turbulence are thus not identical. For flat ‘white-noise’ spectra $E \simeq \text{const}$ the (weak)

magnetic field does not affect the turbulence intensity while the rotation leads to an ‘anti-quenching’ of the transverse turbulence intensity $\langle u_x^2 \rangle$. On the other hand, for spectra E which are steep enough both effects are suppressing (‘quenching’) the turbulence. This finding does not change for $\nu \neq \eta$, see Eq. (37) of [Rüdiger \(1974\)](#).

For the flows parallel to the rotation axis the expression

$$\langle u_z^2 \rangle - \langle u_z^{(0)2} \rangle = \frac{1}{16\pi} \iint \frac{k_x^2 + k_y^2}{k^4}$$

$$\left(\frac{\omega}{(\omega^2 + \eta^2 k^4)^2} \frac{\partial(\omega^2 + \eta^2 k^4)E}{\partial\omega} (2\mathbf{k} \cdot \boldsymbol{\Omega}/k)^2 + \right.$$

$$\left. + \frac{2\omega}{\omega^2 + \eta^2 k^4} \frac{\partial E}{\partial\omega} (\mathbf{k} \cdot \mathbf{V}_A)^2 \right) d\mathbf{k} d\omega \quad (22)$$

results and for the anisotropy caused by rotation and magnetic field

$$\langle u_z^2 \rangle - \langle u_x^2 \rangle = \frac{1}{16\pi} \iint \frac{k_x^2 - k_z^2}{k^4} \frac{\omega}{\omega^2 + \eta^2 k^4}$$

$$\left(\frac{1}{\omega^2 + \eta^2 k^4} \frac{\partial(\omega^2 + \eta^2 k^4)E}{\partial\omega} (2\mathbf{k} \cdot \boldsymbol{\Omega}/k)^2 + \right.$$

$$\left. + 2 \frac{\partial E}{\partial\omega} (\mathbf{k} \cdot \mathbf{V}_A)^2 \right) d\mathbf{k} d\omega, \quad (23)$$

always for $\text{Pm} = 1$. After integration over the wave number components we find

$$\langle u_z^2 \rangle - \langle u_x^2 \rangle = -\frac{1}{60\pi} \iint \frac{\omega}{(\omega^2 + \eta^2 k^4)k^2}$$

$$\left(\frac{2\Omega^2}{\omega^2 + \eta^2 k^4} \frac{\partial(\omega^2 + \eta^2 k^4)E}{\partial\omega} + k^2 V_A^2 \frac{\partial E}{\partial\omega} \right) d\mathbf{k} d\omega \quad (24)$$

for an isotropic spectral function $E = E(k, \omega)$. Indeed, the rotational and the magnetic influences are going in different directions. While the magnetic field supports the vertical turbulence intensity the rotation supports the horizontal intensity. This behavior, which was already suggested by [Chandrasekhar \(1961\)](#), becomes finally clear after inspection of the relation

$$\langle u_z^2 \rangle - \langle u_x^2 \rangle = \frac{\Omega^2}{15\pi} \iint \frac{k}{\omega^2 + \eta^2 k^4} \frac{\partial}{\partial k} \left(\frac{E}{k^2} \right) d\mathbf{k} d\omega, \quad (25)$$

equivalent to the rotation-induced part in (24). As the wave number derivative in (25) is certainly negative it follows $\langle u_x^2 \rangle > \langle u_z^2 \rangle$. This is opposite to the influence of magnetic fields in (24) which runs with $-\partial E/\partial\omega > 0$ hence reducing the horizontal flow components compared with the vertical ones. On the other hand, it can be shown with the expression (18), that for $\Omega \rightarrow \infty$ or $V_A \rightarrow \infty$ always $\langle u_z^2 \rangle = 2\langle u_x^2 \rangle$ ([Rüdiger 1974](#)). In both cases, for sufficiently rapid rotation or strong magnetic field, the vertical turbulence intensity exceeds the transverse intensity by a factor of two.

Magnetic fluctuations also contribute to the magnetic pressure (13). Horizontal isotropy implies that we only have to

compute $\langle b_z^2 \rangle$. To the first order in B_0^2 one finds the simple relation

$$\langle b_z^2 \rangle = \frac{B_0^2}{120\pi} \iint \frac{E}{\omega^2 + \eta^2 k^4} d\mathbf{k} d\omega, \quad (26)$$

so that after (13) the pressure difference between the magnetic and non-magnetic turbulence is

$$\frac{\delta P^{\text{tot}}}{\rho} = \frac{V_A^2}{2} \left(1 - \frac{1}{30\pi} \iint \frac{7\eta^2 k^4 - 9\omega^2}{(\omega^2 + \eta^2 k^4)^2} E(k, \omega) d\mathbf{k} d\omega \right). \quad (27)$$

The turbulence part in this expression does *not* have a definite sign.

Equation (27) may also be written as

$$\frac{\delta P^{\text{tot}}}{\rho} = (1 - \kappa_P) \frac{V_A^2}{2}, \quad (28)$$

hence

$$P_{\text{in}} = P_{\text{ext}} - (1 - \kappa_P) \rho \frac{V_A^2}{2}, \quad (29)$$

Without turbulence $\kappa_P = 0$, see Eq. (1). Positive κ_P reduces the pressure difference. If even $\kappa_P > 1$ the inner gas pressure exceeds the outer one (Kleeorin et al. 1989). On the other hand, anti-quenching of the turbulence by the magnetic field leads to negative κ_P which amplifies the magnetic suppression of the inner gas pressure (Roberts & Soward 1975).

Positive κ_P are a necessary condition for the occurrence of a negative-pressure effect. We have thus mainly to discuss the sign of κ_P which basically depends on the form of the spectral function E . For $\text{Pm} = 1$ one finds

$$\kappa_P = \frac{1}{30\pi} \iint \frac{7\eta^2 k^4 - 9\omega^2}{(\omega^2 + \eta^2 k^4)^2} E(k, \omega) d\mathbf{k} d\omega \quad (30)$$

or, what is the same,

$$\kappa_P = -\frac{1}{30\pi} \iint \left(\frac{7\omega}{\omega^2 + \eta^2 k^4} \frac{\partial E}{\partial \omega} + \frac{2\omega^2 E}{(\omega^2 + \eta^2 k^4)^2} \right) d\mathbf{k} d\omega. \quad (31)$$

Negative values of δP^{tot} require large positive values of κ_P which is only possible for very steep $E(k, \omega)$ as a function of ω . For a steep function such as $\delta(\omega)$ the integral is positive and can even lead to negative δP^{tot} for small magnetic Reynolds numbers

$$\text{Rm}' = \frac{u_{\text{rms}} \ell_{\text{corr}}}{\eta} \quad (32)$$

of the turbulence ('low-conductivity limit').

The two terms in Eq. (31) are easy to understand. The first one certainly vanishes for 'white noise' ($E \simeq \text{const}$) and the second one comes from the positive-definite contribution of the Maxwell stress (26). For the white-noise spectrum the

total pressure excess (28) *cannot* become negative. Similarly, we expect the integral in (30) to be negative for small values of η . In the high-conductivity limit, $\eta \rightarrow 0$,

$$\int_0^\infty \frac{7\eta^2 k^4 - 9\omega^2}{(\omega^2 + \eta^2 k^4)^2} E(k, \omega) d\omega = -\frac{\pi}{2\eta k^2} E(k, 0), \quad (33)$$

hence the leading term of κ_P is negative² so that always $\delta P^{\text{tot}}/\rho > V_A^2/2$.

Hence, in the quasilinear approximation a negative turbulent pressure excess can only exist in the low-conductivity limit if η is not too small. The value of κ_P is negative in the high-conductivity limit and it is positive in the low-conductivity limit. Only in the latter case the negative-pressure effect can appear. More exactly speaking, the total turbulent pressure excess can only be negative for $\text{Rm}' < \pi^2 w_0^*$ if, in the sense of the mixing length theory, $\tau_{\text{corr}} \simeq \ell_{\text{corr}}/u_{\text{rms}}$. We have shown earlier with simplified spectral functions that the characteristic value of w_0^* is of the order of 10 for $\text{Pm} \simeq 1$ (Rüdiger et al. 2012a). For large magnetic Reynolds numbers Rm' of the fluctuations, the integral (30) becomes negative and the effective pressure is enhanced rather than reduced. The bottom plot of Fig. 8 in Kemel et al. (2012) demonstrates the decrease of positive κ_P of increasing Rm' (for forced turbulence).

It remains to consider $\text{Pm} \neq 1$ for which Eq. (30) turns into

$$\kappa_P = \frac{1}{30\pi} \iint \frac{((8\eta - \nu)\nu k^4 - 9\omega^2)E}{(\omega^2 + \nu^2 k^4)(\omega^2 + \eta^2 k^4)} d\mathbf{k} d\omega. \quad (34)$$

It is clearly negative-definite for $\text{Pm} \geq 8$. For large magnetic Prandtl number, therefore, the pressure grows by the turbulence. For all Pm it also grows for flat spectra such as white noise as i

$$\int_0^\infty \frac{(8\eta - \nu)\nu k^4 - 9\omega^2}{(\omega^2 + \nu^2 k^4)(\omega^2 + \eta^2 k^4)} d\omega = -\frac{\pi}{2\eta k^2} \quad (35)$$

is negative-definite. The flat parts of the spectrum thus always *increase* the magnetic-induced pressure. SOCA provides negative pressure excesses only for $\text{Pm} < 8$ and for low enough electric conductivities. After (34) κ_P is positive if the frequency spectrum contains a delta function $\delta(\omega)$ (and $\text{Pm} < 8$) and it is always negative for white noise. For a certain spectrum between the considered two extremes the κ_P will change its sign.

3. ROTATING MAGNETOCONVECTION

One of the results of the foregoing Section is the strong dependence of the integrals for P^{tot} on the form of the spectral function of the turbulence or, what is the same, on the

² $E(k, 0)$ vanishes only for undamped waves

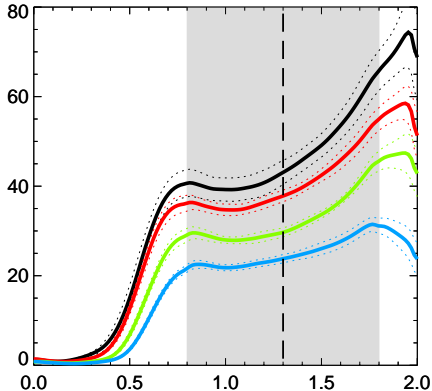


Figure 1. The influence of the molecular Prandtl number Pr on the turbulent pressure (13) in units of $(c_{ac}/100)^2$ without rotation and magnetic field. $Pr = 0.1$ (blue), $Pr = 0.05$ (green), $Pr = 0.02$ (red) and $Pr = 0.01$ (black). The dashed vertical line marks the center of the unstable domain in z where the blue curve yields a minimum value of $Rm' \simeq 40$, the values for the other models are slightly higher. $\Omega^* = B^* = 0$.

ratio of the diffusion time scales. Numerical simulations are needed for further insights. We thus perform simulations for magnetoconvection for various amplitudes of the magnetic field, the ordinary Prandtl number $Pr = \nu/\chi$ (with χ the thermal diffusion coefficient) and the magnetic Prandtl number $Pm = \nu/\eta$. The field B_0 is assumed as vertical and homogeneous. The simulations are done with the NIRVANA code by Ziegler (2002), which uses a conservative finite difference scheme in Cartesian coordinates. The length scale is defined by the depth of the convectively unstable layer. We assume an ideal, fully ionized gas heated from below and keep a fixed temperature at the top of box. Periodic boundary conditions are formulated in the horizontal plane. The upper and lower boundaries are impenetrable and stress-free. The initial state is convectively unstable in the upper half of the box. Convection sets in if the Rayleigh number exceeds its critical value. The model complies with that of Käpylä et al. (2012) with the main difference of the orientation of the mean magnetic field. As in Kitiashvili et al. (2010) and Käpylä et al. (2016) our field is vertically directed while Käpylä et al. (2012) work with horizontal mean magnetic fields.

The velocity field is measured in units of $c_{ac}/100$. This quantity is also used to define the magnetic field via $B_z = B^* \sqrt{\mu_0 \rho_0} c_{ac}/100$. In this normalization $B^* = 1$ represents 1 kG if $c_{ac} = 10$ km/s and $\rho_0 \simeq 10^{-2}$ g/cm³ are adopted. With the equipartition field $B_{eq} = \sqrt{\mu_0 \rho_0} u_{rms}$ it is

$$\frac{B_z}{B_{eq}} = \frac{B^* c_{ac}}{100 u_{rms}}, \quad (36)$$

so that for $u_{rms} = c_{ac}$ the parameter $B^* = 10$ describes the moderate field strength $B_z = 0.1 B_{eq}$. $B^* = 10$ for subsonic

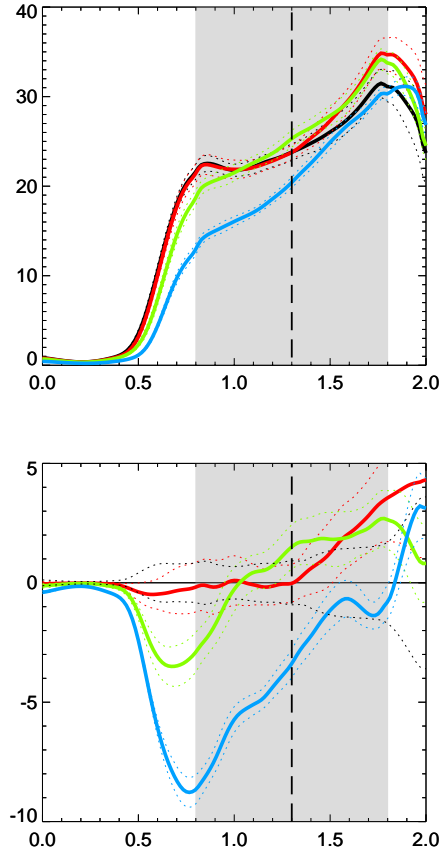


Figure 2. The turbulent pressure $\langle u_x^2 \rangle$ (top) and its excess $\delta P^{tot}/\rho = \langle u_x^2 \rangle - \langle u_x^{(0)2} \rangle$ (bottom) of rotating convection in units of $(c_{ac}/100)^2$. Only the blue line is the result of rotational quenching while the red and the green lines stand for rotational anti-quenching. Pressure is rotationally anti-quenched for slow rotation and it is quenched only for rapid rotation. $\Omega^* = 0$ (black), $\Omega^* = 1$ (red), $\Omega^* = 3$ (green) and $\Omega^* = 10$ (blue). $B^* = 0$, $Pr = 0.1$.

turbulence with $u_{rms} = 0.1 c_{ac}$ stands for equipartition, $B_z = B_{eq}$. We shall often use in what follows $B^* = 10$ as the value of the prescribed background field.

By the units of the vertical size D of the convection box and the convective velocity the rotation is normalized by the relation $\Omega = \Omega^* c_{ac}/100 D$. If the correlation time of the turbulence is written as $\tau_{corr} = \hat{\tau} D/(c_{ac}/100)$ then $\Omega^* \simeq \Omega \tau_{corr}/\hat{\tau}$. We shall demonstrate with simulations that $\hat{\tau} \simeq 0.1 - 0.2$. With the solar values $c_{ac} \simeq 10$ km/s and $D \simeq 200.000$ km the result is $\Omega^* \simeq 4$.

The combination of the rotation rate and the magnetic field yields the magnetic Mach number

$$Mm = \frac{\Omega^*}{B^*} \quad (37)$$

as a normalized rotation rate which in astrophysical applications often exceeds unity. Galaxies have $Mm \lesssim 10$, for the

solar tachocline with a magnetic field of 1 kG one obtains $Mm \simeq 30$, and for typical white dwarfs and neutron stars $Mm \simeq 1000$ (except magnetars).

Also the cores of cold molecular clouds have large magnetic Mach numbers. Polarization measurements of magnetic fields in cloud cores indicate that the cores are filled by magnetic fields of a few μG (Li et al. 2009). Velocity measurements indicate rotation rates $\Omega \simeq 10^{-13}\text{s}^{-1}$ for cloud cores with a radius of 0.1 pc (Burkert & Bodenheimer 2000; Klaassen et al. 2009). With the typical density 10^5cm^{-3} one finds $Mm \simeq 5$.

On the other hand, for stellar material the heat-conductivity χ is the dominant diffusivity (Hanasoge et al. 2016). It is thus the Roberts number $q = \chi/\eta = \text{Pm}/\text{Pr} \gg 1$. Large q mimic large electric conductivities if the heat-conductivity is fixed. Characteristic values are $\text{Pm} \simeq 6 \cdot 10^{-2}$ and $\text{Pr} \simeq 2 \cdot 10^{-6}$ so that $q = O(10^4)$ for the bottom of the solar convection zone (see Ossendrijver (2003); Gough (2007)). Close to the solar surface the Roberts number becomes smaller but remains larger than unity.

3.1. Rotating convection

We start to compute the reference pressure of the model without rotation and magnetic field after (13). By use of the same numerical model Rüdiger et al. (2012b) in their Fig. 6 found for weak magnetic field that $u_{\text{rms}} \simeq 9$ for the normalized turbulence intensity leading to pressure values of $\simeq 27$. This value is perfectly fitted by the data given in Fig. 1. The lines represent a large number of snapshots with low scattering. There is a clear anticorrelation of turbulence intensity and Prandtl number Pr . The smaller the ordinary Prandtl number the larger is the Mach number of the convection.

Figure 2 demonstrates the influence of the rotation on the horizontal turbulence intensity $\langle u_x^2 \rangle$ of the thermal convection which simultaneously represents its mean-field pressure. The black solid line of the top plot gives the averaged quantity of Fig. 1. This curve is anti-quenched by slow rotation and it is quenched for rapid rotation just as it was discussed below Eq. (21) for driven turbulence within the quasilinear theory. We take this result as a strong motivation for further applications of the SOCA theory also for rotating MHD models. The bottom panel displays the same numerical models with respect to the difference $\langle u_x^2 \rangle - \langle u_x^{(0)2} \rangle$ which gives the excess of turbulent pressure with respect to the non-rotating convection. Negative values describe the rotational quenching of the turbulence intensity by the rotation while positive values describe a support of $\langle u_x^2 \rangle$. The latter happens for slow rotation (red and green lines, $\langle u_x^2 \rangle > \langle u_x^{(0)2} \rangle$) while for rapid rotation with $\langle u_x^2 \rangle < \langle u_x^{(0)2} \rangle$ the opposite is true.

The total pressure by rotating convection is the sum of the turbulence-originated pressure $\langle u_x^2 \rangle$ and the centrifugal pressure $\Omega^2 R^2 / 2D^2$ by the global solid-body rotation (in code

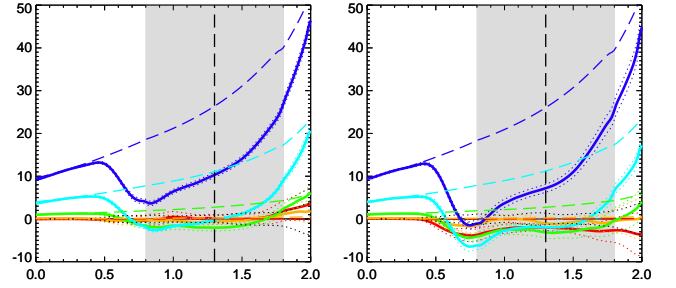


Figure 3. The pressure excess $\delta P^{\text{tot}}/\rho$ for vertical background field with $B^* = 1$ (yellow), $B^* = 3$ (red) and $B^* = 10$ (green), $B^* = 20$ (light blue) and $B^* = 30$ (dark blue). Negative values stand for $P_{\text{in}} > P_{\text{ext}}$ while positive values stand for the standard relation $P_{\text{in}} < P_{\text{ext}}$, see Eq. (1). The dashed lines give the pressure excess without turbulence in the same units as used in Fig. 1. The vertical dashed line marks the center of the unstable box at $z = 1.3$ where the pressure excess is minimal for $B^* = 10$. $\Omega^* = 0$, $\text{Pm} = 0.1$, $\text{Pr} = 0.1$ (left), $\text{Pr} = 0.05$ (right).

units). Obviously, for slow rotation the pressure term $\langle u_x^2 \rangle$ does not ‘feel’ the rotation but it is (slightly) reduced if it is fast. In the latter case the effective pressure is smaller than $\langle u_x^{(0)2} \rangle$ plus centrifugal term.

3.2. Magnetoconvection

The turbulence intensity $\langle u^2 \rangle$ for $B^* = 10^{-3}$ and $B^* = 1$ has been computed without rotation by Rüdiger et al. (2012b) without remarkable differences of the two models. The influence of vertical magnetic fields upon the pressure should thus be negligible for $B^* < 1$. This is indeed shown by the red line of Fig. 3. Magnetic fields must exceed $B^* \simeq 1$ in order to influence the convective pressure remarkably. However, fields with $B^* > 1$ indeed reduce the magnetic pressure (1) without turbulence. Figure 3 gives the pressure excess (28) without rotation for vertical background fields with $B^* \leq 30$. Negative values stand for negative pressure excesses, $P_{\text{in}} > P_{\text{ext}}$, which appear for both the given Prandtl numbers for moderate B^* green and light blue lines). The Prandtl numbers are similar to those used by Käpylä et al. (2012).

In order to exclude boundary effects we focus attention to the values around the central line at $z = 1.3$ (vertical dashed lines). For comparison the dashed lines give the pressure excess *without turbulence* in the same units as used in Fig. 1. They represent the solution of Dicke in Eq. (1). Because of the density stratification the curves are *not* strictly horizontal³. Values of the pressure excess below the dashed lines stand for magnetic pressure suppression ($\kappa_P > 0$) while val-

³ the normalized initial density is set to unity at the upper boundary of the unstable layer

ues above the dashed lines reflect magnetic-induced pressure amplification ($\kappa_P < 0$). In all cases plotted in Fig. 3 a distinct reduction of the large-scale magnetic pressure by the turbulence within the unstable zone appears independent of the Prandtl number. For strong fields with $B^* > 20$, however, the amplitudes are no longer large enough to generate negative values of the pressure excesses. The figure demonstrates the existence of a maximal magnetic field strength of about $B^* = 20$ for the negative-pressure effect. For stronger fields the turbulence-free magnetic term in (1) can never be over-compensated by the turbulence quenching. With the limiting value $B^* = 20$ the ratio of the magnetic energy to the kinetic energy is $\simeq 0.4$ (see Fig. 1). One finds that the turbulence can indeed reduce this value or can even change the sign of $\delta P^{\text{tot}}/\rho$. After the second relation in (1) also the temperature excess would then change its sign and in the magnetized domain becomes bright rather than dark.

In the simulations by Käpylä et al. (2012) where for weak fields the turbulence always leads to negative magnetic-pressure effect the ordinary Prandtl number is fixed to $\text{Pr} = 1$. In our models decreasing Prandtl numbers imply decreasing magnetic resistivity η : the values in code units are $\eta = 0.063$ for $\text{Pr} = 0.1$ and $\eta = 0.044$ for $\text{Pr} = 0.05$. The locations of the lines, however, do hardly depend on the value of the ordinary Prandtl number. In all cases the fields with $B^* = 10$ lead to a significant *amplification* of the inner molecular pressure by about 7%. We shall show, however, that under the influence of a global rotation these models loose their negative performance. For weaker magnetic fields the effects are weaker.

3.3. Rotating magnetoconvection

So far the modification of Eq. (1) under the presence of rotating or magnetized turbulence has been considered. The natural next question is that after the structure of rotating *and* magnetized turbulence. Equations (10)–(12) form the expressions for the numerical simulations. The combined influences of magnetic field and rigid rotation with parallel Ω , B and $\nabla\rho$ are probed for slow and rapid rotation.

After Fig. 3 the nonrotating models with $B^* = 10$ (green lines) provide the largest negative turbulent pressure excesses. We shall thus use this value in order to study the rotational influence. It is known from Fig. 2 that rotation amplifies the horizontal turbulence intensity hence we expect the lines for $\Omega^* \neq 0$ to be shifted upwards in comparison with the red lines for $\Omega^* = 0$. This is indeed the result of the simulations shown in the plots of Fig. 4 for two values of the ordinary Prandtl number. The rotation over-compensates the negative-pressure effect which for $\Omega^* \gtrsim 10$ starts to disappear. Hence, for $\text{Mm} = 1$ it is in the center of the box $\delta P^{\text{tot}} \simeq 0$. Hence, if the magnetic background field is parallel to the rotation axis the interaction of magnetic field and

rotation keeps the resulting differences of gas pressure for magnetic and non-magnetic convection as rather small.

The calculations are more complicated for rotating magnetoconvection if a finite angle exists between the magnetic field and the rotation axis. One should believe that the effective rotation rate for the convective box with vertical magnetic field is reduced by the factor $\cos\theta$ but this is only one side of the medal. On the other hand, it is also true that the magnetized oblique rotator generates a turbulence field which is anisotropic also in the horizontal (x, y) plane. The numerical simulations provide a rather clear picture. Figure 5 shows the results for inclination angles $\theta = 30^\circ$ (left panel) and $\theta = 45^\circ$ (right panel). In both cases for rapid rotation (bottom plots) the lines for the three magnetic field amplitudes proceed to positive values. The negative-pressure effect also disappears for rapid rotation, therefore, when the magnetic axis and the rotation axis are not parallel.

3.4. Rapid rotation, $\text{Mm} > 1$

It remains to study the pressure differences in rapidly rotating convection with magnetic Mach numbers exceeding unity. Our model works with $\Omega^* = 30$ with $B^* = 1$, $B^* = 3$ and $B^* = 10$ so that the magnetic Mach number is $\text{Mm} > 1$ reaching values up to 30. Figure 6 demonstrates how the pressure excess goes to zero for increasing magnetic Mach number both for $\theta = 0^\circ$ and for $\theta = 30^\circ$. In these cases, therefore, Eq. (2) simplifies to $P_{\text{in}} \simeq P_{\text{ext}}$ despite the existence of large-scale magnetic fields. The explanation of the darkness of sunspots by the mean Lorentz force inside the spot domain, if real, could work for rapid rotation. Also the opposite assumption of negative pressure excess inside the sunspot (and possible resulting instabilities) does not hold for rapid rotation. For fast rotating turbulence the sum of Reynolds stress and Maxwell stress does not depend on the strength of the (moderate) magnetic field. The total pressure does thus not depend on the magnetic field (if $B^* \leq 10$), it always equals the pressure without magnetic field. Weak and moderate fields do neither reduce nor enhance the turbulence pressure, with respect to the pressure the magnetic field is hidden by the turbulence.

If starspots of similar structure exist for both slow rotation and rapid rotation then the turbulence-originated negative magnetic-pressure excess can not be essential for the spot-formation.

4. CONCLUSIONS

The total pressure in a rotating and/or magnetized convection is considered where mostly the rotation axis, the magnetic field and the density gradient are parallel. We start to discuss the anisotropies originated by rotation or by magnetic field for driven turbulence in a quasilinear approach. Often the results of such analytic correlation approximation

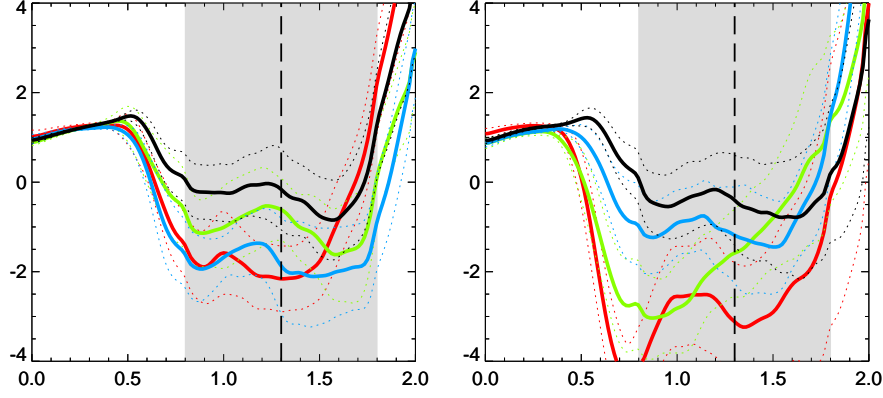


Figure 4. Rotating magnetoconvection with $Mm < 1$ for $\theta = 0^\circ$: pressure excess $\delta P^{\text{tot}}/\rho$ after Eq. (28) for $\Omega^* = 0$ (red), $\Omega^* = 1$ (green), $\Omega^* = 3$ (blue) and $\Omega^* = 10$ (black) for vertical background field with $B^* = 10$. Negative values stand for magnetic quenching while positive values stand for anti-quenching. $Pm = 0.1$. $Pr = 0.1$ (left), $Pr = 0.05$ (right).

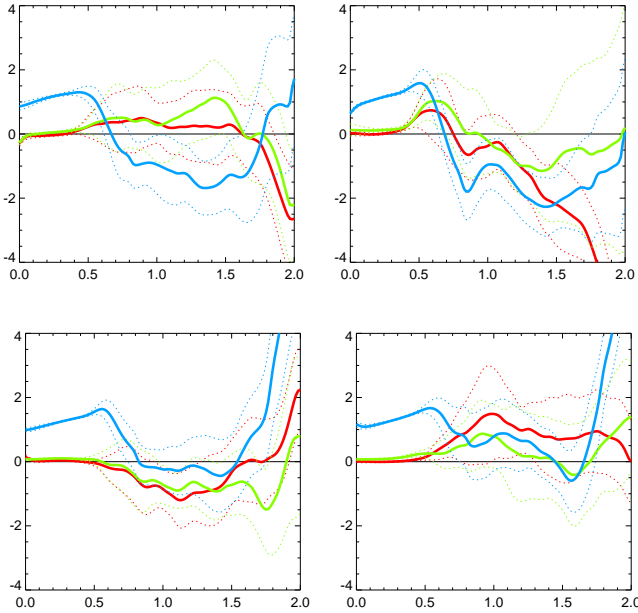


Figure 5. The total pressure excess $\delta P^{\text{tot}}/\rho$ for vertical background field $B^* = 1$ (red), $B^* = 3$ (green), $B^* = 10$ (blue) for oblique rotation with $\theta = 30^\circ$ (left) and $\theta = 45^\circ$ (right). Top: $\Omega^* = 1$, bottom: $\Omega^* = 10$. $Pm = Pr = 0.1$.

are confirmed by direct numerical simulations but we also have to look for possible differences. Note that the quasilinear approach only deals with driven turbulence.

If the driven turbulence is isotropic without rotation it is anisotropic with rotation in the sense that the turbulence intensity transverse to the rotation axis exceeds the turbulence intensity along the rotation axis. We find the opposite anisotropy for driven turbulence subject to a uniform axial magnetic field. It is thus not surprising that the turbulent pressure (by the Reynolds stress) for rotation exceeds the tur-

bulent pressure without rotation and again the opposite is true for the influence of axial magnetic fields, see Eq. (21).

However, the total pressure in turbulence under the influence of magnetic fields is formed not only by the Reynolds stress but also by the Maxwell stress where the latter is combined by a large-scale and a small-scale part. All together form the total pressure excess $\delta P^{\text{tot}} = P^{\text{tot}}(B) - P^{\text{tot}}(0)$ which in equilibrium equals the gas pressure difference without and with magnetic field. Without turbulence δP^{tot} is positive (almost) by definition, see Eq. (1). It is confirmed that for turbulence under the influence of weak magnetic fields δP^{tot} can be negative which phenomenon is called the negative magnetic-pressure effect (Brandenburg et al. 2010, 2011, 2012).

One finds from the SOCA approximation for driven turbulence that for weak fields this effect should not exist for large Pm . Moreover, for $Pm < 8$ upper bounds of the magnetic Reynolds number of the turbulence exist to allow negative δP^{tot} . For higher magnetic Reynolds numbers, however, it is always $\delta P^{\text{tot}} > 0$. The negative magnetic-pressure effect can thus only exist for rather low values of the molecular electric conductivity. For the high-conductivity limit with $\mu_0 \sigma \ell_{\text{corr}}^2 \gg \tau_{\text{corr}}$ the turbulence-originated pressure enhances the large-scale magnetic pressure $B_0^2/2\mu_0$ rather than to reduce it. For decreasing Prandtl number Pr the magnetic-free turbulence intensity slightly grows (Fig. 1) while simultaneously for the MHD models the molecular η sinks.

For the model of the lowest curve in Fig. 1 we have computed the correlation time by means of its autocorrelation function. The result is $\hat{\tau} \simeq 0.1$ in code units. Hence $\eta_T \simeq \langle u_x^2 \rangle \hat{\tau} \simeq 2.5$ taken in the middle of the convection box. For the correlation length it results $\ell_{\text{corr}} \simeq \sqrt{\langle u_x^2 \rangle} \hat{\tau} \simeq 0.5$. In the average, the box contains two eddies in the vertical dimension. With $\eta = 0.063$ taken from Section 3.2 one finds

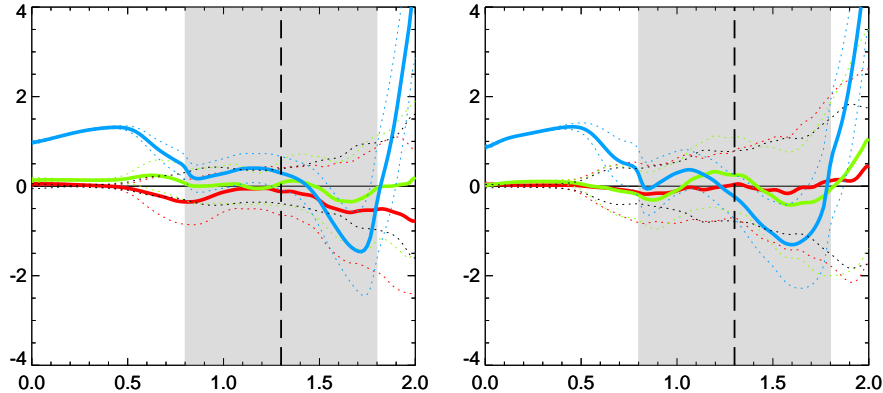


Figure 6. Rapidly-rotating magnetoconvection with $Mm > 1$ for $\theta = 0^\circ$ (left) and $\theta = 30^\circ$ (right). Pressure excess $\delta P^{\text{tot}}/\rho$ after Eq. (28) for $\Omega^* = 30$. $B^* = 1$ (red), $B^* = 3$ (green) and $B^* = 10$ (blue). The pressure excess almost completely disappears. $Pm = 0.1$, $Pr = 0.1$.

$\eta_T/\eta \simeq 40$ as a proxy of the magnetic Reynolds number Rm' of the fluctuations.

For vertical fields it is even possible to derive the eddy diffusivity η_T directly from the simulations. We have shown earlier that convection subject to uniform magnetic fields provides a finite cross correlation $\langle \mathbf{u} \cdot \mathbf{b} \rangle$ proportional to the scalar product $\mathbf{B} \cdot \nabla \rho$ (Rüdiger et al. 2012b). It vanishes for homogeneous turbulence and for fields perpendicular to the density stratification. The quasilinear approximation and numerical simulations lead to

$$\langle u_z b_z \rangle = -\eta_T \frac{B_0}{H_\rho}, \quad (38)$$

where H_ρ as the density scale height is here about 1.4 in code units for all models. We have computed the correlation (38) in the middle plane of the convective box averaging over the horizontal plane and time. The resulting eddy diffusivity values for $B^* = 3$ and $B^* = 10$ are almost identical for one and the same model. We find $\eta_T/\eta \simeq 30$ for both $Pr = 0.1$ and $Pr = 0.05$ close to the above given approximative result. For $Pr < 0.05$ the reliability of the simulations with our code was only restricted.

It remains to report the influence of rapid rotation to the low-conductivity case where the negative magnetic-pressure effect for moderate fields always exists. Figure 4 demonstrates that it is erased by the basic rotation. For $Mm > 1$ the pressure differences between magnetic and non-magnetic fluids are completely planished (Fig. 6). For large rotation rates it is always $P^{\text{tot}}(B) \simeq P^{\text{tot}}(0)$ so that the influence of the (weak) magnetic field disappears. For all fields the sum of turbulent pressure and magnetic pressure (the large scale contribution included) remains constant and does not depend on the magnetic field amplitude.

It is often argued that large-scale magnetic fields and turbulence are supporting cold molecular clouds against self-gravity and the external pressure. The star formation rate seems to be lowered by the magnetic pressure so that only a few percent of the mass of the molecular cloud reaches a stellar configuration. The observed large-scale magnetic fields are of order $30 \mu\text{G}$ on scales of 0.1-10 pc (Crutcher 1999). On the other hand, the angular momentum transport by the Lorentz force (Dorfi 1982) and/or magnetic quenching of the turbulence (Zamora-Avilés et al. 2018) may increase the star formation rate. Our result that for large magnetic Mach numbers the total pressure (combined by turbulence plus small-scale magnetic fields plus large-scale magnetic field) always equals its non-magnetic value excludes a basic magnetic influence on the star formation rate as long as the magnetic field is weak. It is not finally clear, however, if it is allowed to transmit the properties of rotating convection to other forms of turbulence.

Another open question is whether not only the magnetic-originated diagonal elements of the tensor (4) but also its off-diagonal elements vanish for rapid rotation. Of particular interest are the terms with one of the indices representing ϕ (in spherical coordinates) which describe the angular momentum transport by magnetic fields and turbulence. One can show that the angular momentum transport by rotating density-stratified turbulence vanishes for $\Omega^* \rightarrow \infty$ even under the presence of an azimuthal magnetic field (Kitchatinov et al. 1994) but the consequences of fast-rotating turbulence for the magnetic braking by the background Lorentz force are still unknown.

REFERENCES

Brandenburg, A., Kemel, K., Kleeorin, N., Mitra, D., & Rogachevskii, I. 2011, *ApJL*, 740, L50, doi: [10.1088/2041-8205/740/2/L50](https://doi.org/10.1088/2041-8205/740/2/L50)

Brandenburg, A., Kemel, K., Kleeorin, N., & Rogachevskii, I. 2012, *The Astrophysical Journal*, 749, 179, doi: [10.1088/0004-637X/749/2/179](https://doi.org/10.1088/0004-637X/749/2/179)

- Brandenburg, A., Kleeorin, N., & Rogachevskii, I. 2010, *Astronomische Nachrichten*, 331, 5, doi: [10.1002/asna.200911311](https://doi.org/10.1002/asna.200911311)
- Burkert, A., & Bodenheimer, P. 2000, *The Astrophysical Journal*, 543, 822, doi: [10.1086/317122](https://doi.org/10.1086/317122)
- Chandrasekhar, S. 1961, *Hydrodynamic and hydromagnetic stability* (Oxford: Clarendon)
- Crutcher, R. M. 1999, *The Astrophysical Journal*, 520, 706, doi: [10.1086/307483](https://doi.org/10.1086/307483)
- Dicke, R. H. 1970, *The Astrophysical Journal*, 159, 25, doi: [10.1086/150287](https://doi.org/10.1086/150287)
- Dorfi, E. 1982, *Astronomy & Astrophysics*, 114, 151
- Gough, D. 2007, in *The Solar Tachocline*, ed. D. W. Hughes, R. Rosner, & N. O. Weiss, 3
- Hanasoge, S., Gizon, L., & Sreenivasan, K. R. 2016, *Annual Review of Fluid Mechanics*, 48, 191, doi: [10.1146/annurev-fluid-122414-034534](https://doi.org/10.1146/annurev-fluid-122414-034534)
- Käpylä, P. J., Brandenburg, A., Kleeorin, N., Käpylä, M. J., & Rogachevskii, I. 2016, *Astronomy & Astrophysics*, 588, A150, doi: [10.1051/0004-6361/201527731](https://doi.org/10.1051/0004-6361/201527731)
- Käpylä, P. J., Brandenburg, A., Kleeorin, N., Mantere, M. J., & Rogachevskii, I. 2012, *Month. Not. Roy. Astr. Soc.*, 422, 2465, doi: [10.1111/j.1365-2966.2012.20801.x](https://doi.org/10.1111/j.1365-2966.2012.20801.x)
- Kemel, K., Brandenburg, A., Kleeorin, N., Mitra, D., & Rogachevskii, I. 2012, *SoPh*, 280, 321, doi: [10.1007/s11207-012-9949-0](https://doi.org/10.1007/s11207-012-9949-0)
- Kitchatinov, L. L., Rüdiger, G., & Küker, M. 1994, *Astronomy & Astrophysics*, 292, 125
- Kitiashvili, I. N., Kosovichev, A. G., Wray, A. A., & Mansour, N. N. 2010, *The Astrophysical Journal*, 719, 307, doi: [10.1088/0004-637X/719/1/307](https://doi.org/10.1088/0004-637X/719/1/307)
- Klaassen, P. D., Wilson, C. D., Keto, E. R., & Zhang, Q. 2009, *The Astrophysical Journal*, 703, 1308, doi: [10.1088/0004-637X/703/2/1308](https://doi.org/10.1088/0004-637X/703/2/1308)
- Kleeorin, N. I., Rogachevskii, I. V., & Ruzmaikin, A. A. 1989, *Pisma v Astronomicheskii Zhurnal*, 15, 639
- Li, H.-b., Dowell, C. D., Goodman, A., Hildebrand, R., & Novak, G. 2009, *The Astrophysical Journal*, 704, 891, doi: [10.1088/0004-637X/704/2/891](https://doi.org/10.1088/0004-637X/704/2/891)
- Losada, I. R., Brandenburg, A., Kleeorin, N., & Rogachevskii, I. 2013, *Astronomy & Astrophysics*, 556, A83, doi: [10.1051/0004-6361/201220939](https://doi.org/10.1051/0004-6361/201220939)
- Losada, I. R., Warnecke, J., Glogowski, K., et al. 2017, *ArXiv e-prints*. <https://arxiv.org/abs/1704.04062>
- Ossendrijver, M. 2003, *A&A Rv*, 11, 287, doi: [10.1007/s00159-003-0019-3](https://doi.org/10.1007/s00159-003-0019-3)
- Roberts, P. H., & Soward, A. M. 1975, *Astronomische Nachrichten*, 296, 49, doi: [10.1002/asna.19752960202](https://doi.org/10.1002/asna.19752960202)
- Rüdiger, G. 1974, *Astronomische Nachrichten*, 295, 275
- Rüdiger, G., Kitchatinov, L. L., & Hollerbach, R. 2013, *Magnetic Processes in Astrophysics: theory, simulations, experiments* (Wiley-VCH)
- Rüdiger, G., Kitchatinov, L. L., & Schultz, M. 2012a, *Astronomische Nachrichten*, 333, 84, doi: [10.1002/asna.201111635](https://doi.org/10.1002/asna.201111635)
- Rüdiger, G., Küker, M., & Schnerr, R. S. 2012b, *Astronomy & Astrophysics*, 546, A23, doi: [10.1051/0004-6361/201219268](https://doi.org/10.1051/0004-6361/201219268)
- Zamora-Avilés, M., Vázquez-Semadeni, E., Körtgen, B., Banerjee, R., & Hartmann, L. 2018, *Month. Not. Roy. Astr. Soc.*, 474, 4824, doi: [10.1093/mnras/stx3080](https://doi.org/10.1093/mnras/stx3080)
- Ziegler, U. 2002, *Astronomy & Astrophysics*, 386, 331, doi: [10.1051/0004-6361:20020126](https://doi.org/10.1051/0004-6361:20020126)